European Journal of Radiology Open 3 (2016) 153–161

European Journal of Radiology Open

journal homepage: www.elsevier.com/locate/ejro

Fiber tracking: A qualitative and quantitative comparison between four different software tools on the reconstruction of major white matter tracts

Foteini Christidi[a], Efstratios Karavasilis[b], Kostantinos Samiotis[c], Sotirios Bisdas[d], Nikolaos Papanikolaou[e,*]

[a] 1st Department of Neurology, Aeginition Hospital, Medical School, National and Kapodistrian University, Athens, Greece
[b] 2nd Department of Radiology, University General Hospital 'Attikon', School of Medicine, National and Kapodistrian University of Athens, Athens, Greece
[c] Research and Development, Papanikolaou N & Associates, Heraklion, Greece
[d] Department of Neuroradiology, The National Hospital for Neurology and Neurosurgery, University College London Hospitals, London, UK
[e] Centre for the Unknown, Champalimaud Foundation, Lisbon, Portugal

ARTICLE INFO

Article history:
Received 22 May 2016
Received in revised form 22 June 2016
Accepted 23 June 2016
Available online 18 July 2016

Keywords:
Deterministic tractography
Fiber tracking
Diffusion tensor imaging
Magnetic resonance imaging

ABSTRACT

Purpose: Diffusion tensor imaging (DTI) enables in vivo reconstruction of white matter (WM) pathways. Considering the emergence of numerous models and fiber tracking techniques, we herein aimed to compare, both quantitatively and qualitatively, the fiber tracking results of four DTI software (Brainance, Philips FiberTrak, DSI Studio, NordicICE) on the reconstruction of representative WM tracts.
Materials and methods: Ten healthy participants underwent 30-directional diffusion tensor imaging on a 3T-Philips Achieva TX MR-scanner. All data were analyzed by two independent sites of experienced raters with the aforementioned software and the following WM tracts were reconstructed: corticospinal tract (CST); forceps major (Fmajor); forceps minor (Fminor); cingulum bundle (CB); superior longitudinal fasciculus (SLF); inferior fronto-occipital fasciculus (IFOF). Visual inspection of the resulted tracts and statistical analysis (inter-rater and betweensoftware agreement; paired *t*-test) on fractional anisotropy (FA), axial and radial diffusivity (Daxial, Dradial) were applied for qualitative and quantitative evaluation of DTI software results.
Results: Qualitative evaluation of the extracted tracts confirmed anatomical landmarks at least for the core part of each tract, even though differences in the number of fibers extracted and the whole tract were evident, especially for the CST, Fmajor, Fminor and SLF. Descriptive values did not deviate from the expected range of values for healthy adult population. Substantial inter-rater agreement (intraclass correlation coefficient [ICC], Bland-Altman analysis) was found for all tracts (ICC; FA: 0.839–0.989, Daxial: 0.704–0.991, Dradial: 0.972–0.993). Low agreement for FA, Daxial and Dradial (ICC; Bland-Altman analysis) and significant paired *t*-test differences ($p < 0.05$) were detected regarding between-software agreement.
Conclusions: Qualitative comparison of four different DTI software in addition to substantial inter-rater but poor between-software agreement highlight the differences on existing fiber tracking methodologies and several particularities of each WM tract, further supporting the need for further study in both clinical and research settings.

1. Introduction

Diffusion-weighted magnetic resonance imaging (DW-MRI) is based on the random coherent motion of water molecules, utilizing it as a contrast mechanism in order to quantify the anisotropic diffusion corresponding to the anatomical structure of the human brain [1]. In the brain, diffusion is restricted by the various tissue structures and can therefore be used to investigate its microstructure.

* Corresponding author. Current address: Centre for the Unknown, Champalimaud Foundation, Avenida Brasília, 1400-038 Lisbon, Portugal.
E-mail addresses: npapan@npapan.com, nikolaos.papanikolaou@fundacaochampalimaud.pt (N. Papanikolaou).

http://dx.doi.org/10.1016/j.ejro.2016.06.002

Diffusion tensor imaging (DTI) [2] constitutes a formal description of the aforementioned relation. In regions where the principal diffusion direction concurs with the major eigenvector of the diffusion ellipsoid [3], following the local orientation allows in-vivo reconstruction of fiber bundles [4–6] via various single-tensor tractography approaches [7] (Fiber Assignment by Continuous Tracking (FACT), Streamline, TENsor Deflection (TEND) algorithms).

However, the traditional single-tensor DTI-based tractography, which is mainly extracting all the directional information about the fiber from the major eigenvector, has been proven limited. In this case, DTI orientation estimates have a direct anatomical meaning only in regions where there is no fiber crossing/kissing/fanning/branching and only a single bundle of parallel axons runs through a voxel of the image. When more complex patterns are observed, such as within-voxel fiber crossing, the correlation of the model estimates to the anatomical gold standard is less straightforward [4,8]. More sophisticated approaches have therefore been developed.

The emergence of numerous models and fiber tracking techniques during the past decade raises the need for a comprehensive and quantitative comparison between different software and, thus, different implemented tracking methodologies. In the present study, we compare, on both qualitative and quantitative way, the fiber tracking results of four different DTI software: Brainance (*Advantis Medical Imaging, Eindhoven, The Netherlands*), Philips FiberTrak (*Philips, Best, The Netherlands*), DSI Studio [9], NordicICE (*Nordic NeuroLab, Bergen, Norway*).

2. Material and methods

2.1. Study design

Ten healthy right-handed volunteers (4 males) aged between 22 and 42 years old (M = 31.50 years; SD = 7.09 years) were included in the study. All participants gave their informed consent to be scanned for the research purpose of the study, which were done in accordance to the declaration of Helsinki and had been approved by the Local Ethical Committee. Inclusion criterion was age older than 18 years old. Exclusion criteria were (a) presence of any neurological condition affecting central nervous system (CNS); (b) severe psychiatric illness or other systemic disease; (c) psychoactive drugs or other medication that could affect CNS; (d) alcohol or drug abuse; (e) known structural pathology in the MRI and (f) standard contraindications for MRI. Neurological conditions, severe psychiatric illness or other systemic diseases were excluded based on interview of each participant before scanning, including detailed assessment of each participant's available medical records for excluding possible medication treatment with known effects on CNS. The absence of any brain pathology was further confirmed by experienced radiologists based on participants' MRI scanning.

2.2. MR imaging acquisition

All participants underwent brain MRI examination on a 3T system (Achieva TX; Philips, Best, The Netherlands) using an 8-channel SENSE head coil.

2.2.1. 3D T1-weighted acquisition

The T1-weighted sequence was acquired using a three-dimensional sequence (time of repetition (TR): 9.9 ms, echo time (TE): 3.7 ms, flip angle: 7°, voxel-size $1 \times 1 \times 1$ mm, sagittal slice orientation, matrix size 244×240).

2.2.2. DTI acquisition

DTI acquisition included an axial single-shot spin-echo echo-planar imaging sequence with 30 diffusion encoding directions and the following parameters: TR: 7299 ms, TE: 68 ms, flip angle: 90°, field of view: 256×256 mm, acquisition voxel size: $2 \times 2 \times 2$ mm, sensitivity encoding reduction factor of 2, two b factors with 0 s/mm^2 (low b), and 1000 s/mm^2 (high b) with two b factors averaged per b value, in order to ensure better signal-to-noise ratio (SNR). The acquisition consisted of 70 slices and the scan time was 8 min 40 s.

2.3. DTI tractography analysis

The following WM tracts were examined as representative of projection, commissural, and associative WM fibers: corticospinal tract (CST); forceps major (Fmajor); forceps minor (Fminor); cingulum bundle (CB); superior longitudinal fasciculus (SLF); inferior fronto-occipital fasciculus (IFOF).

For the tract reconstruction we used four different fiber tracking software available to the raters, whose description can be found below:

2.3.1. Brainance DTI suite (Advantis Medical Imaging, Eindhoven, The Netherlands)

Brainance DTI software suite is a cloud-based tool developed by *Advantis Medical Imaging* towards a more efficient, robust and anatomically accurate fiber tractography and quantification result. In *Brainance*, a new fiber tracking methodology has been developed and implemented, mostly based on the principles of the deterministic logic, which is highly accurate in the final 3D reconstruction of the fiber bundles in comparison to the anatomical gold standard.

2.3.2. FiberTrak package (Philips, Best, The Netherlands)

FiberTrak is a DTI software package developed by Philips which implements the Fiber Assignment with Continuous Tracking (FACT) algorithm in order to reconstruct the fiber pathways.

2.3.3. DSI studio (http://dsi-studio.labsolver.org)

DSI Studio is a non-commercial software for diffusion MR images analysis. The provided functions include reconstruction, deterministic fiber tracking (TEND algorithm) and 3D visualization.

2.3.4. NordicICE (Nordic NeuroLab, Bergen, Norway)

The *NordicICE* Diffusion/DTI Module generates diffusion maps from MR diffusion imaging studies from all major MR vendors. It also includes the feature of reconstructing fiber tracts (Fiber Tracking) in the CNS and can quantify fiber statistics such as fractional anisotropy (FA), apparent diffusion coefficient (ADC) and more. The parametric values that are shown correspond to the selected output maps that were generated during the DTI analysis.

During the selection of the region-of-interest (ROI) in all the aforementioned software, a multiple ROI approach was applied for the reconstruction of the CST according to well-known anatomical landmarks. We selected three primary ROIs on axial slices: (a) the bundle of fibers running in the rostrocaudal axial in the anterior pons; (b) the posterior limbs of the internal capsule; and (c) the precentral gyrus. Fmajor, Fminor, CB, SLF and IFOF tracts were reconstructed according to previously published protocols [10]. All reconstructed fibers that are transpassing all ROIs were included. The fiber tracking procedure was performed with the thresholds of minimum FA value at 0.15, and maximum angle at 27°. Mean FA, axial (Daxial) and radial (Dradial) diffusivities were calculated by each software, except for *NordicICE* where only mean FA measurements were performed for the reconstructed fiber bundles due to the available software release limitations.

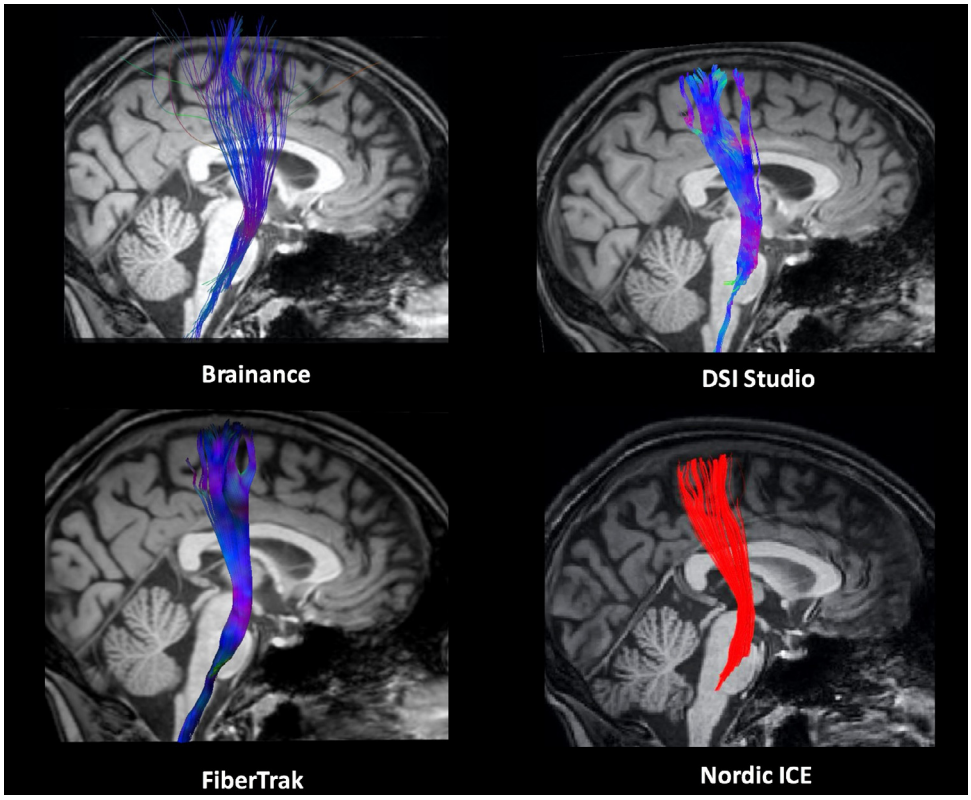

Fig. 1. Reconstruction of the left corticospinal tract overlaid on a high-resolution T1-3D sagittal slice using Brainance (upper left); DSI studio (upper right); Philips FiberTrak (bottom left); NordicICE (bottom right).

2.4. Measurements of agreement

Two independent sites (site A: raters E.K., F.C.; site B: rater K.S.) performed DTI analysis with both *Brainance* and their own available DTI suites.

2.4.1. Inter-rater agreement

To determine inter-rater agreement in the tracts of interest (CST; Fmajor; Fminor; CB; SLF; IFOF) *Brainance* was used and all DTI datasets were analyzed. All raters worked independently, were blinded to the results of each other and had dedicated knowledge in DTI analysis.

2.4.2. Between-software agreement

Site A had access to *Philips FiberTrak* and site B had access to *DSI Studio* and *NordicICE*. To determine between-software agreement in the tracts of interest, a comparison between the DTI parameters calculated from *Brainance* and each one of the other software was conducted (i.e. site A: *Brainance* vs. *FiberTrak*; site B: *Brainance* vs. *DSI Studio*; *Brainance* vs. *NordicICE*).

2.5. Statistical analysis

Mean value of FA, Daxial and Dradial for all studied tracts were automatically extracted from the selected DTI software packages. Inter-rater agreement was assessed within the group of 10 participants for all DTI parameters (mean FA; mean Daxial; mean Dradial) with intraclass correlation coefficient (ICC) [11]. ICC values were interpreted according to the following convention for agreement [11]: 0.00–0.10 = virtually none; 0.11–0.40 = slight; 0.41–0.60 = fair; 0.61–0.80 = moderate; 0.81–1.00 = substantial agreement. Negative ICC values can be observed, providing evidence of poor agreement [12]. For between-software agreement, we further applied Bland-Altman analysis [13], where the difference in paired DTI parameters (mean FA; mean Daxial; mean Dradial) was plotted against the average from the two readings (i.e. site A: *Brainance* vs FiberTrak; site B: *Brainance* vs. *DSI Studio*; *Brainance* vs. *NordicICE*). The coefficients of variability for each DTI parameter, indicating the greatest difference between measurements in 95% of paired observations, were calculated as r = 1.96 × SD (dif)/mean (standard deviation of the difference between paired observations divided by their mean). In addition, to assess between-software agreement for the tracts of interest, we used two-tailed paired *t*-test and the level of significance was set at $p < 0.05$. All statistical analyses were conducted using the MedCalc ® (version 16.2.0).

3. Results

3.1. Qualitative analysis

3.1.1. CST

The reconstructed CST (Fig. 1) runs along the major anatomical landmarks that is anterior pons, internal capsule and precentral gyrus. We observed between-software differences in the CST tracts considering the reconstruction of fibers originated from the motor cortex (using the *Brainance* software) and the visualization of crossing CST fibers at the level of the pons (using the *DSI Studio* and especially the *Brainance* software).

3.1.2. Fmajor, Fminor

The reconstruction of the callosal radiations at the occipital (Fmajor) and frontal (Fminor, Fig. 2) lobes did not reveal any significant differences with regards to the core anatomical landmarks for the tracts, with the only exception being the number of reconstructed fibers, specifically for the Fmajor.

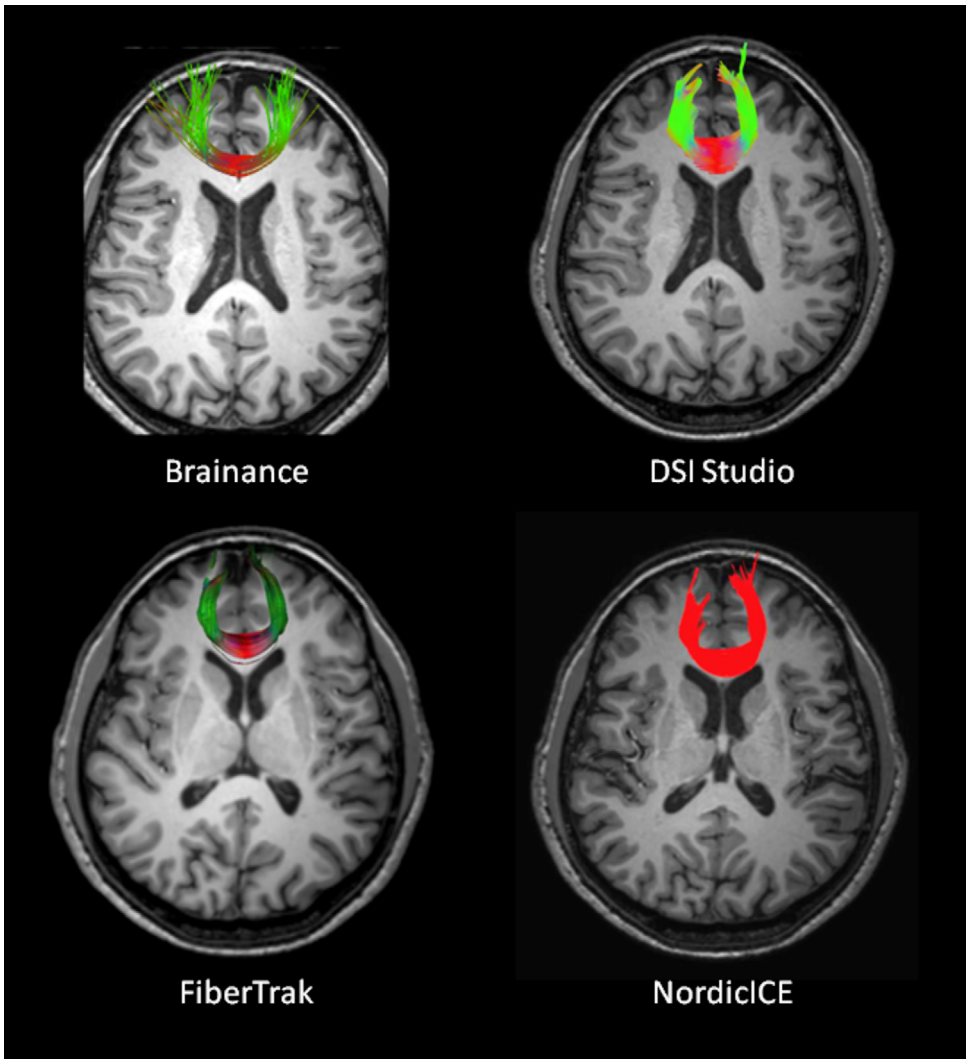

Fig. 2. Reconstruction of the forceps minor overlaid on a high-resolution T1-3D axial slice using Brainance (upper left); DSI studio (upper right); Philips FiberTrak (bottom left); NordicICE (bottom right).

3.1.3. CB

We identified the anatomical landmarks of the CB bilaterally that lies within cingulate gyrus and extends from the frontal lobe, around the rostrum and the genu of the CC, continues above the body of the CC, before curving ventrally around the splenium of the CC. Differences regarding the most anterior and posterior fibers of the CB can be detected in the reconstructed tracts from the four different software (Fig. 3). In the present study, we did not include the cingulum-parahippocampal part.

3.1.4. SLF

The SLF bilaterally is identified at the caudal part of the superior temporal gyrus, arches around the sylvian fissure and continues forward to end within the frontal lobe. The subcomponents of the SLF can be identified in most but not all reconstructed SLF tracts.

3.1.5. IFOF

The major anatomical landmarks for the IFOF bilaterally can be visualised in the reconstructed tracts for both left and right hemisphere. The resulted tract runs posteriorly from prefrontal cortical areas and at the junction of the frontal and temporal lobes, it narrows passing through the anterior floor of the external capsule, continuing then posteriorly and terminating in the middle and inferior gyri of the temporal lobe and in the occipital lobe. Differences in the number of reconstructed tracts and the anterior part of the IFOF are evident by visual inspection of the reconstructed tracts by the four software (Fig. 4).

3.2. Quantitative analysis

Tables 1–3 present descriptive values (mean, SD, min-max) for the DTI metrics (FA, Daxial, Dradial) extracted by the aforementioned DTI software for each tract of interest. Quantitative analysis on Daxial and Dradial was applied and presented only for *Brainance*, *FiberTrak* and *DSI Studio*, as previously described.

3.2.1. Inter-rater agreement

The inter-rater agreement (agreement between rater 1, 2, and 3 for *Brainance*) is shown in Table 4. Overall, the inter-rater agreement was substantial for most of the WM tracts and DTI metrics, with ICCs ranging between 0.839–0.989 for FA, 0.704–0.991 for Daxial and 0.972–0.993 for Dradial.

3.2.2. Between-software agreement

Table 5 presents ICC indices and r% for between-software agreement comparisons between *Brainance* and *FiberTrak* (separately for each rater from site A with full access to both suites), *Brainance* and *DSI Studio* and finally *Brainance* and *NordicICE*. ICCs

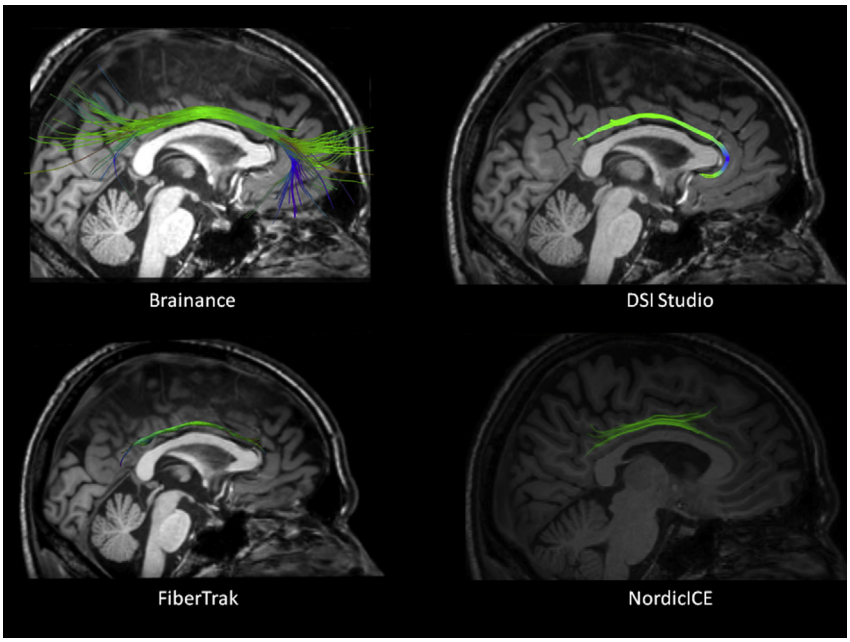

Fig. 3. Reconstruction of the left cingulum bundle overlaid on a high-resolution T1-3D sagittal slice using Brainance (upper left); DSI studio (upper right); Philips FiberTrak (bottom left); NordicICE (bottom right).

for mean FA, mean Daxial and Dradial were extremely low for the majority of tracts of interest. The Bland-Altman analysis indices further indicated that there was virtually poor or no agreement between software packages. Moderate to substantial agreement was observed for the following tracts and specific DTI values: CST-R (Dradial: *Brainance* vs *DSI Studio*), Fmajor (Dradial: *Braiinance* vs *DSI Studio*), Fminor (FA: *Brainance* vs *NordicICE*; Daxial: *Brainance* vs *FiberTrak*), CB-L (FA: *Brainance* vs *FiberTrak*, *Brainance* vs *NordicICE*; Daxial, Dradial: *Brainance* vs *FiberTrak*), CB-R (Dradial: *Brainance* vs *DSI Studio*), SLF-L (FA: *Brainance* vs *NordicICE*; Dradial: *Brainance* vs *FiberTrak*), SLF-R (FA: *Brainance* vs *DSI Studio*; Dradial: *Brainance* vs *DSI Studio*), IFOF-R (*Brainance* vs *DSI Studio*). Between-software agreement using ICC and Bland-Altman analysis was further supported by paired *t*-test comparisons between pairs of software, revealing significant between-software differences ($p < 0.05$) in the majority of tracts of interest, with the exception being the between-software differences (*Brainance vs. FiberTrak*) on Daxial and Dradial (Table 6).

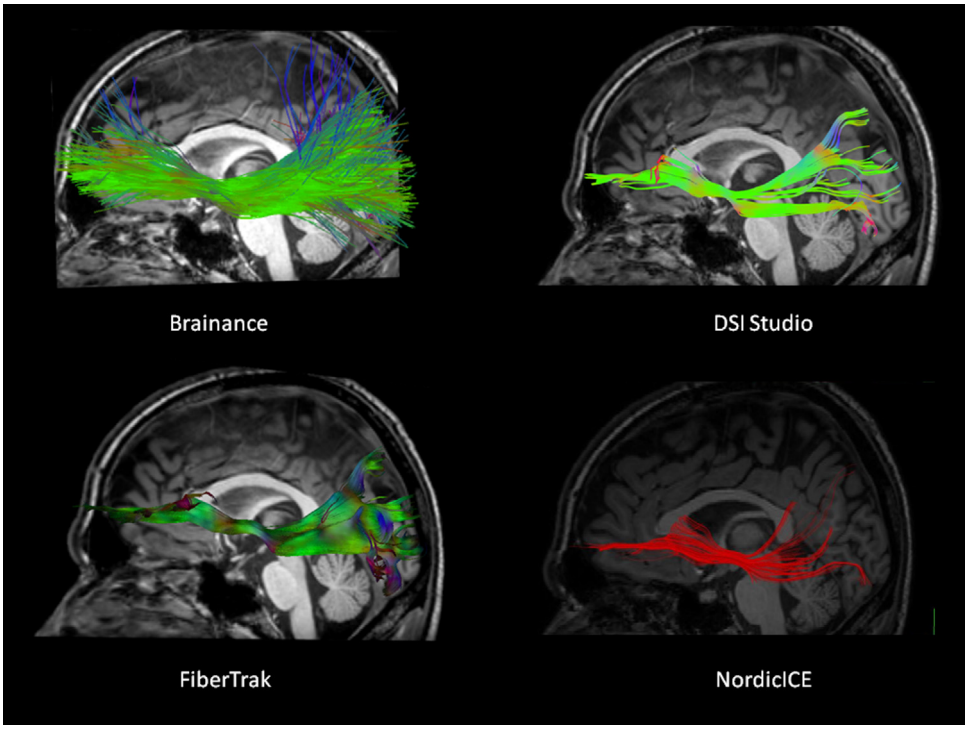

Fig. 4. Reconstruction of the left inferior fronto-occipital fasciculus overlaid on a high-resolution T1-3D sagittal slice using Brainance (upper left); DSI studio (upper right); Philips FiberTrak (bottom left); NordicICE (bottom right).

Table 1
Descriptive statistics for FA parameter extracted by each software for tracts of interest.

Tract of interest	DTI software															
	Brainance				FiberTrak				DSI Studio				NordicICE			
	Mean	SD	Min	Max	Mean	SD	Min	Max	Mean	SD	Min	Max	Mean	SD	Min	Max
CST-L	0.531	0.012	0.509	0.549	0.528	0.02	0.503	0.563	0.586	0.014	0.56	0.605	0.542	0.024	0.497	0.571
CST-R	0.535	0.02	0.498	0.568	0.503	0.019	0.478	0.538	0.57	0.011	0.555	0.587	0.521	0.017	0.504	0.564
Fmajor	0.577	0.023	0.543	0.612	0.51	0.032	0.46	0.569	0.641	0.017	0.62	0.678	0.541	0.02	0.503	0.547
Fminor	0.462	0.02	0.428	0.485	0.427	0.014	0.405	0.446	0.534	0.021	0.495	0.558	0.459	0.021	0.422	0.487
CB-L	0.43	0.025	0.401	0.479	0.431	0.023	0.39	0.463	0.549	0.027	0.5	0.585	0.466	0.026	0.408	0.485
CB-R	0.45	0.031	0.406	0.49	0.393	0.021	0.367	0.44	0.503	0.034	0.439	0.557	0.413	0.029	0.37	0.478
SLF-L	0.425	0.019	0.4	0.455	0.427	0.019	0.402	0.463	0.5	0.019	0.462	0.525	0.436	0.02	0.405	0.472
SLF-R	0.461	0.019	0.428	0.487	0.408	0.022	0.373	0.44	0.467	0.024	0.427	0.508	0.397	0.018	0.369	0.427
IFOF-L	0.454	0.02	0.43	0.495	0.45	0.016	0.423	0.474	0.517	0.016	0.499	0.553	0.42	0.024	0.388	0.463
IFOF-R	0.466	0.015	0.449	0.491	0.428	0.014	0.411	0.459	0.502	0.017	0.474	0.536	0.398	0.013	0.38	0.423

Table 2
Descriptive statistics for Daxial metric extracted by each software for tracts of interest.

Tract of interest	DTI software															
	Brainance				FiberTrak				DSI Studio				NordicICE			
	Mean	SD	Min	Max	Mean	SD	Min	Max	Mean	SD	Min	Max	Mean	SD	Min	Max
CST-L	1.302	0.045	1.228	1.356	1.257	0.038	1.19	1.31	1.265	0.029	1.216	1.316	n/a			
CST-R	1.252	0.045	1.15	1.306	1.283	0.043	1.205	1.33	1.322	0.045	1.237	1.402	n/a			
Fmajor	1.441	0.036	1.4	1.501	1.44	0.046	1.37	1.51	1.556	0.103	1.345	1.69	n/a			
Fminor	1.295	0.032	1.256	1.358	1.284	0.028	1.24	1.335	1.399	0.073	1.329	1.583	n/a			
CB-L	1.165	0.033	1.116	1.219	1.153	0.024	1.11	1.19	1.287	0.027	1.217	1.31	n/a			
CB-R	1.178	0.019	1.147	1.206	1.13	0.029	1.09	1.185	1.244	0.036	1.187	1.288	n/a			
SLF-L	1.143	0.031	1.089	1.185	1.136	0.021	1.11	1.165	1.181	0.021	1.151	1.22	n/a			
SLF-R	1.155	0.024	1.124	1.191	1.14	0.032	1.09	1.19	1.171	0.013	1.153	1.188	n/a			
IFOF-L	1.32	0.028	1.287	1.365	1.251	0.03	1.19	1.285	1.312	0.022	1.289	1.351	n/a			
IFOF-R	1.258	0.022	1.23	1.298	1.263	0.036	1.21	1.33	1.323	0.042	1.278	1.413	n/a			

Table 3
Descriptive statistics for Dradial metric extracted by each software for tracts of interest.

Tract of interest	DTI software															
	Brainance				FiberTrak				DSI Studio				NordicICE			
	Mean	SD	Min	Max	Mean	SD	Min	Max	Mean	SD	Min	Max	Mean	SD	Min	Max
CST-L	0.525	0.022	0.493	0.565	0.523	0.039	0.475	0.588	0.447	0.017	0.432	0.478	n/a			
CST-R	0.506	0.021	0.469	0.542	0.56	0.037	0.485	0.608	0.489	0.029	0.439	0.54	n/a			
Fmajor	0.502	0.034	0.461	0.554	0.599	0.066	0.498	0.685	0.488	0.024	0.455	0.52	n/a			
Fminor	0.581	0.024	0.551	0.62	0.639	0.024	0.605	0.675	0.538	0.024	0.509	0.579	n/a			
CB-L	0.576	0.026	0.543	0.619	0.566	0.024	0.535	0.605	0.49	0.027	0.447	0.524	n/a			
CB-R	0.555	0.03	0.515	0.595	0.6	0.021	0.55	0.628	0.529	0.034	0.482	0.59	n/a			
SLF-L	0.574	0.026	0.535	0.622	0.577	0.024	0.543	0.618	0.517	0.025	0.479	0.566	n/a			
SLF-R	0.545	0.023	0.51	0.585	0.595	0.023	0.565	0.645	0.545	0.029	0.493	0.592	n/a			
IFOF-L	0.56	0.037	0.502	0.622	0.593	0.013	0.568	0.61	0.542	0.02	0.491	0.559	n/a			
IFOF-R	0.572	0.023	0.532	0.6	0.631	0.035	0.575	0.685	0.572	0.043	0.505	0.662	n/a			

Table 4
Intraclass correlation coefficient (ICC) for *Brainance* inter-rater agreement.

DTI parameters	WM tracts-of-interest									
	CST-L	CST-R	Fmajor	Fminor	CB-L	CB-R	SLF-L	SLF-R	IFOF-L	IFOF-R
FA	0.893	0.948	0.839	0.989	0.969	0.964	0.984	0.965	0.986	0.98
Daxial	0.925	0.981	0.704	0.991	0.866	0.71	0.976	0.95	0.956	0.889
Dradial	0.921	0.93	0.94	0.972	0.972	0.98	0.993	0.976	0.935	0.993

4. Discussion

One of the major advantages of the diffusion tensor fiber tracking techniques is that they can potentially give information about in vivo brain connectivity through the mapping of the WM anatomy. This technique is difficult to be validated, as far as the accuracy rates of the reconstruction are concerned, due to our limited knowledge regarding the human brain and the lack of a gold standard. However, studies which have initially been implemented on artificial data (phantoms), tried to expand on human brain data (with realistic noise levels) and quantify the accuracy achieved in the depiction of WM structure [14,15]. They found that the accuracy rates from the deterministic approaches lie at around 55–60% [16], due to the methodologies' failure to tackle the problem of the crossing, branching, kissing phenomena and precisely depict the termination points of the fibers [17]. The other category of fiber

Table 5
Intraclass correlation coefficient (ICC) and Bland-Altman analysis for the between-software agreement.

Tract of interest	DTI parameter	Brainance vs. FiberTrak				Brainance vs. DSI		Brainance vs. NordicICE	
		Rater EK		Rater FC		Rater KS		Rater KS	
		ICC	r (%)	ICC	r (%)	ICC	r (%)	ICC	r (%)
CST-L	FA	0.263	8.054	0.241	9.767	−0.101	−1.652	−0.961	9.708
	Daxial	0.563	8.58	0.406	9.847	0.519	9.725	n/a	
	Dradial	0.537	12.01	0.517	13.704	0.037	29.02	n/a	
CST-R	FA	−0.335	18.448	−0.503	17.791	−0.03	2.559	−0.898	14.686
	Daxial	0.425	5.383	0.403	5.759	0.485	0.417	n/a	
	Dradial	0.248	2.573	0.207	3.431	0.641	13.193	n/a	
Fmajor	FA	−0.058	32.963	−0.041	31.066	0.09	−7.394	0.551	9.551
	Daxial	−0.176	9.888	0.037	8.684	0.208	13.267	n/a	
	Dradial	−0.166	12.238	−0.137	8.906	0.769	9.549	n/a	
Fminor	FA	0.4	13.689	0.352	13.737	0.217	−11.707	0.923	5.014
	Daxial	0.68	5.267	0.646	5.242	0.106	2.632	n/a	
	Dradial	0.36	−4.995	0.287	−6.17	0.469	12.782	n/a	
CB-L	FA	0.763	9.81	0.687	10.518	0.127	−17.499	0.875	0.966
	Daxial	0.771	5.282	0.731	5.438	0.103	−5.905	n/a	
	Dradial	0.726	9.5	0.67	9.583	0.237	23.012	n/a	
CB-R	FA	0.2	27.637	0.082	29.092	0.413	1.116	0.421	21.918
	Daxial	−0.188	10.764	0.027	10.112	0.096	0.252	n/a	
	Dradial	0.189	5.026	0.094	3.107	0.632	14.73	n/a	
SLF-L	FA	0.287	10.545	0.473	10.919	0.141	−10.956	0.84	1.47
	Daxial	−0.335	7.108	−0.714	7.59	−0.03	3.885	n/a	
	Dradial	0.717	7.786	0.746	7.187	0.285	18.804	n/a	
SLF-R	FA	0.022	25.15	−0.061	26.218	0.805	4.575	0.201	21.536
	Daxial	−0.848	9.721	−0.935	9.295	0.022	2.278	n/a	
	Dradial	0.231	−1.241	0.19	0.175	0.886	7.066	n/a	
IFOF-L	FA	−0.278	13.046	0.265	11.983	0.185	−7.776	0.446	17.894
	Daxial	0.457	5.287	0.524	4.664	0.176	−0.943	n/a	
	Dradial	0.481	7.845	0.487	8.027	0.447	18.982	n/a	
IFOF-R	FA	0.008	18.057	0.028	17.502	0.291	−1.771	0.11	14.229
	Daxial	0.074	4.728	0.328	3.342	0.015	0.483	n/a	
	Dradial	0.169	1.036	0.16	−0.16	0.738	10.217	n/a	

tracking algorithms, the probabilistic ones, which are currently only used at a limited extent when it comes to clinical practice, achieve much higher accuracy rates [18].

In addition, fiber tracking reliability depends on the quality of the data and the robustness of the algorithms used, as well as from the effects of various anatomical and image acquisition parameters like SNR, anisotropy, curvature, background anisotropy, step size, and interpolation [19]. In general, fiber tracking with common deterministic algorithms (i.e. FACT) with high SNR and high anisotropy using interpolation and a low step size gives the most reliable results. Partial volume effects are shown to have a detrimental effect when the background is anisotropic and when tracking narrows fibers [19].

In the present study, the fiber tracking results of two variants of the FACT algorithm (*FiberTrak, Nordic ICE and DSI Studio*) with a novel deterministic one (*Brainance)* were compared. To this direction, we chose to reconstruct representative WM tracts of projection, associative and commissural fiber system and used anatomical-based protocols with high reproducibility [10] and multiple ROI approach for fiber tracking. A visual inspection and qualitative evaluation of the extracted tracts from the different programs confirmed anatomical landmarks for the tracts of interest at least for the core part of each tract [20], even though differences in the number of fibers extracted and the whole tract are evident, especially for the CST, the callosal radiations (i.e. Fmajor and Fminor), the IFOF, and the SLF.

CST was included as the most representative projection bundle from motor cortex to the pons through the posterior limbs of the internal capsule. All algorithms were able to reconstruct the CST along its trajectory. Visual evaluation of the resulted tracts further revealed the extraction of fibers lateral to the core CST tract (foot CST) at the level of the precentral gyrus/motor cortex both in left and right hemisphere using the *Brainance*, with these fibers possibly representing the CST of the hand, as well as both ipsilateral and contralateral CST fibers at the level of the pons [21] (Fig. 1). The reconstruction of the callosal radiations over the occipital and frontal lobes (i.e. Fmajor and Fminor, respectively) did not reveal any deviations from the already known anatomical

Table 6
P-values for the calculated DTI parameters regarding the between-software comparison.

Tract of interest	FA				Daxial				Dradial			
	S1 vs. S2	S1 vs. S3	S1 vs. S4	S3 vs. S4	S1 vs. S2	S1 vs. S3	S1 vs. S4	S3 vs. S4	S1 vs. S2	S1 vs. S3	S1 vs. S4	S3 vs. S4
CST-L	0.782	<0.001	0.231	<0.001	0.007	0.005	n/a	n/a	1	<0.001	n/a	n/a
CST-R	0.002	0.002	0.114	<0.001	0.097	0.001			0.001	0.127		
Fmajor	0.002	<0.001	0.001	<0.001	0.441	<0.001			0.006	0.006		
Fminor	<0.001	<0.001	0.979	<0.001	0.349	0.002			<0.001	<0.001		
CB-L	0.659	<0.001	0.001	<0.001	0.09	<0.001			0.149	<0.001		
CB-R	0.014	<0.001	0.001	<0.001	0.006	<0.001			0.005	0.029		
SLF-L	0.81	<0.001	0.003	<0.001	0.655	0.021			0.685	<0.001		
SLF-R	<0.001	0.068	<0.001	<0.001	0.251	0.031			<0.001	0.482		
IFOF-L	0.644	<0.001	<0.001	<0.001	0.964	<0.001			0.426	0.001		
IFOF-R	<0.001	<0.001	<0.001	<0.001	0.17	<0.001			<0.001	0.831		

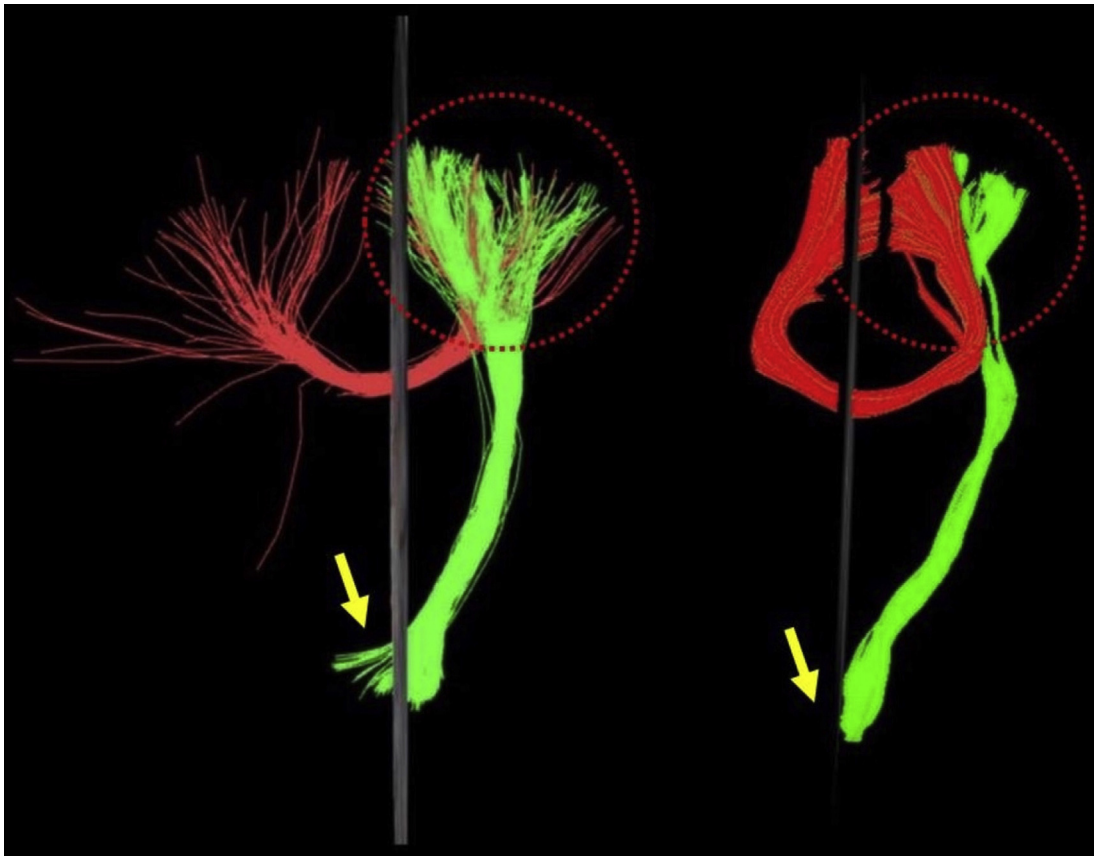

Fig. 5. Comparison between Brainance and FACT algorithms on disclosing crossing fibers of callosal radiations and CST (dashed circle). The FACT algorithm rendered significantly fewer fibers, while Brainance was able to depict crossing diagonal located fibers of both corpus callosum and CST (lateral branches). In addition, Brainance demonstrated decussation of CST fibers in the pons (arrow).

structures (Fig. 2), yet difference in the number of fibers was obvious and it might probably reflect the underlying methodological approach used by each software (i.e. fiber interpolation). Brainance clearly was less sensitive to crossing, kissing fibers problem, as compared to FACT algorithms (DSI Studio) (Fig. 5).

Descriptive values for each tract of interest did not deviate from the expected range of values for healthy adult population [24]. In addition to the qualitative analysis, we included inter-rater and between-software agreement analysis to quantitatively evaluate the tracts of interest and the DTI parameters estimated from the different software. All raters had dedicated knowledge in quantitative DTI analysis and tractography from past research projects. The considerable inter-rater agreement using either ICC or Bland-Altman analysis identifies the accuracy of the used tracking protocols and the validity of the extracted quantitative DTI parameters. With regards to between-software agreement, we found virtually poor agreement with fair to substantial agreement not following a systematic pattern neither among the tracts nor the DTI parameters. Those significant differences in the DTI parameters extracted by the software compared have also been observed in other studies focused either on CNS [16] or peripheral nervous system [25] fiber tracts.

4.1. Limitations and future directions

Despite the fact that we used independent raters, widely-accepted tractography protocols and applied both qualitative and quantitative analysis, the current study is not free of limitations. One of the caveats was the limited sample of DTI data, mostly acquired from young-middle aged healthy volunteers. The statistical strength of the quantitative results can be improved, increasing significantly the size and the age range of the sample. Furthermore, we reconstructed a limited number of WM tracts. We did not include DTI data from CNS pathology (i.e. brain tumor) which would further increase the clinical validity of the extracted WM tracts (i.e. pre-surgical evaluation) and the between-software comparison analysis. In the present study, we also used the default threshold values (FA, angle threshold) for reconstructing representative commissural, associative and projection WM tracts. However, in the future a more optimized methodological approach in a larger sample size including additional WM tracts (i.e. entire corpus callosum; anterior commissure; uncinate fasciculus; inferior longitudinal fasciculus; optic radiation; Meyer loop) would include the proposal of different threshold values for the reconstruction of WM tracts with different curvature characteristics and length size. Another limitation to be mentioned regarding the *Brainance* software is the depiction of fiber tracts as lines and not as tubes due to computational restrictions posed by the users' web browsers. By tackling this issue in the future, the reconstructed fiber tracts will be much more smoothly presented in the 3D space.

5. Conclusion

In this paper, we used both qualitative and quantitative comparison of four fiber tracking software suites and, thus, of four different fiber tracking methodologies regarding their performance at reconstructing some of the major WM tracts. At first, qualitative analysis indicated that although the results show agreement concerning the reconstruction of some fiber bundles (Fmajor, Fminor), smaller or bigger differences are observed when it comes to others (CST, CB,

IFOF and SLF bilaterally). The quantitative analysis confirmed at some point the qualitative results, showing virtually poor or no agreement and fair to substantial agreement not following a systematic pattern neither among the tracts nor the DTI parameters at the between-software comparison. This phenomenon has also been observed at previous studies, and we assume that it reflects the different fiber tracking algorithmic methodologies as well as the aforementioned particularities of each WM fiber bundle.

Conflict of interest

All authors disclose no financial support or involvement in organization(s) with financial interest in the subject matter.

Acknowledgments

We would like to thank all the participants of the present study. We would also like to acknowledge Dr. O. Benekos and Dr. P. Mparas for providing all necessary research keys for sequence acquisition.

References

[1] D. Le Bihan, E. Breton, D. Lallemand, P. Grenier, E. Cabanis, M. Laval-Jeantet, MR imaging of intravoxel incoherent motions: application to diffusion and perfusion in neurologic disorders, Radiology 61 (2) (1986) 401–407.
[2] P.J. Basser, J. Mattiello, D. LeBihan, Estimation of the effective self-diffusion tensor from the NMR spin echo, J. Magn. Reson. B 103 (1994) 247–254.
[3] C. Pierpaoli, P.J. Basser, Toward a quantitative assessment of diffusion anisotropy, Magn. Reson. Med. 36 (1996) 893–906.
[4] P.J. Basser, S. Pajevic, C. Pierpaoli, J. Duda, A. Aldroubi, In vivo fiber tractography using DT-MRI data, Magn. Reson. Med. 44 (4) (2000) 625–632.
[5] T.E. Conturo, N.F. Lori, T.S. Cull, E. Akbudak, A.Z. Snyder, J.S. Shimony, R.C. McKinstry, H. Burton, M.E. Raichle, Tracking neuronal fiber pathways in the living human brain, Proc. Natl. Acad. Sci. 96 (18) (1999) 10422–10427.
[6] S. Mori, B.J. Crain, V.P. Chacko, P.C. Van Zijl, Three-dimensional tracking of axonal projections in the brain by magnetic resonance imaging, Ann. Neurol. 45 (1999) 265–269.
[7] M. Catani, R.J. Howard, S. Pajevic, D.K. Jones, Virtual in vivo interactive dissection of white matter fasciculi in the human brain, Neuroimage 17 (1) (2002) 77–94.
[8] K.K. Seunarine, D.C. Alexander, Multiple fibers: beyond the diffusion tensor, in: H. Johansen-Berg, T. Behrens (Eds.), Diffusion MRI: From Quantitative Measurement to In Vivo Neuroanatomy, Elsevier, 2009, pp. 55–72.
[9] F.C. Yeh, T.D. Verstynen, Y. Wang, J.C. Fernández-Miranda, W.Y.I. Tseng, Deterministic diffusion fiber tracking improved by quantitative anisotropy, PLoS One 8 (11) (2013) e80713.
[10] S. Wakana, A. Caprihan, M.M. Panzenboeck, J.H. Fallon, M. Perry, R.L. Gollub, K. Hua, J. Zhang, H. Jiang, P. Dubey, A. Blitz, P. Van Zijl, S. Mori, Reproducibility of quantitative tractography methods applied to cerebral white matter, Neuroimage 36 (3) (2007) 630–644.
[11] P.E. Shrout, J.L. Fleiss, Intraclass correlations: uses in assessing rater reliability, Psychol. Bull. 86 (2) (1979) 420.
[12] B. Giraudeau, Negative values of the intraclass correlation coefficient are not theoretically possible, J. Clin. Epidemiol. 49 (10) (1996) 1205–1206.
[13] J.M. Bland, D.G. Altman, Statistical methods for assessing agreement between two methods of clinical measurement, Lancet 1 (8476) (1986) 307–310.
[14] T.G. Close, J.D. Tournier, F. Calamante, L.A. Johnston, I. Mareels, A. Connelly, A software tool to generate simulated white matter structures for the assessment of fibre-tracking algorithms, Neuroimage 47 (4) (2009) 1288–1300.
[15] P. Fillard, M. Descoteaux, A. Goh, S. Gouttard, B. Jeurissen, J. Malcolm, A. Ramirez-Manzanares, M. Reisert, K. Sakaie, F. Tensaouti, T. Yo, J.F. Mangin, C. Poupon, Quantitative evaluation of 10 tractography algorithms on a realistic diffusion MR phantom, Neuroimage 56 (May (1)) (2011) 220–234.
[16] G.C. Feigl, W. Hiergeist, C. Fellner, K.M. Schebesch, C. Doenitz, T. Finkenzeller, A. Brawanski, J. Schlaier, Magnetic resonance imaging diffusion tensor tractography: evaluation of anatomical accuracy of different fiber tracking software packages, World Neurosurg. 81 (1) (2014) 144–150.
[17] H.W. Chung, M.C. Chou, C.Y. Chen, Principles and limitations of computational algorithms in clinical diffusion tensor MR tractography, Am. J. Neuroradiol. 32 (1) (2011) 3–13.
[18] M. Bucci, M.L. Mandelli, J.I. Berman, B. Amirbekian, C. Nguyen, M.S. Berger, R.G. Henry, Quantifying diffusion MRI tractography of the corticospinal tract in brain tumors with deterministic and probabilistic methods, NeuroImage Clin. 3 (2013) 361–368.
[19] J.D. Tournier, F. Calamante, M.D. King, D.G. Gadian, A. Connelly, Limitations and requirements of diffusion tensor fiber tracking: an assessment using simulations, Magn. Reson. Med. 47 (4) (2002) 701–708.
[20] M. Catani, M. Thiebau de Schotten, Atlas of Human Brain Connections, Oxford University Press, New York, 2012.
[21] A. Brodal, Neurological Anatomy in Relation to Clinical Medicine, Oxford University Press, New York, 1969.
[24] I.J. Bennett, D.J. Madden, C.J. Vaidya, D.V. Howard, J.H. Howard, Age-related differences in multiple measures of white matter integrity: a diffusion tensor imaging study of healthy aging, Hum. Brain Mapp. 31 (3) (2010) 378–390.
[25] R. Guggenberger, D. Nanz, G. Puippe, K. Rufibach, L.M. White, M.S. Sussman, G. Andreisek, Diffusion tensor imaging of the median nerve: intra-, inter-reader agreement, and agreement between two software packages, Skeletal Radiol. 41 (8) (2012) 971–980.